Journal of Pathology
J Pathol (2011)
Published online in Wiley Online Library
(wileyonlinelibrary.com) DOI: 10.1002/path.2895

ORIGINAL PAPER

Notch3 signalling promotes tumour growth in colorectal cancer

Valentina Serafin,[1†] Luca Persano,[1†] Lidia Moserle,[1†] Giovanni Esposito,[2] Margherita Ghisi,[1] Matteo Curtarello,[2] Laura Bonanno,[1] Massimo Masiero,[1] Domenico Ribatti,[3] Michael Stürzl,[4] Elisabeth Naschberger,[4] Roland S Croner,[5] Adrian M Jubb,[6] Adrian L Harris,[7] Hartmut Koeppen,[8] Alberto Amadori[1,2] and Stefano Indraccolo[2]*

[1] *Department of Oncology and Surgical Sciences, University of Padua, 35128 Padova, Italy*
[2] *Istituto Oncologico Veneto—IRCCS, 35128 Padova, Italy*
[3] *Department of Human Anatomy and Histology, University of Bari Medical School, Bari, Italy*
[4] *Division of Molecular and Experimental Surgery, Department of Surgery, University of Erlangen-Nuremberg, Erlangen, Germany*
[5] *Department of Surgery, University of Erlangen-Nuremberg, Erlangen, Germany*
[6] *Nuffield Department of Clinical Laboratory Sciences, University of Oxford, John Radcliffe Hospital, Headington, Oxford, UK*
[7] *Weatherall Institute of Molecular Medicine, University of Oxford, John Radcliffe Hospital, Headington, Oxford, UK*
[8] *Department of Pathology, Genentech Inc, South San Francisco, CA, USA*

**Correspondence to: Stefano Indraccolo, MD, Istituto Oncologico Veneto—IRCCS, Via Gattamelata 64, 35128 Padua, Italy.*
e-mail: stefano.indraccolo@unipd.it

[†]These authors contributed equally to this work.

Abstract

Increased Notch1 activity has been observed in intestinal tumours, partially accomplished by β-catenin-mediated up-regulation of the Notch ligand Jagged-1. Whether further mechanisms of Notch activation exist and other Notch receptors might be involved is unclear. Microarray data indicated that Notch3 transcript levels are significantly up-regulated in primary and metastatic CRC samples compared to normal mucosa. Moreover, Notch3 protein was expressed at strong/moderate levels by 19.7% of 158 CRC samples analysed, and at weak levels by 51.2% of the samples. Intrigued by these findings, we sought to investigate whether Notch3 modulates oncogenic features of CRC cells. By exploiting xenografts of CRC cells with different tumourigenic properties in mice, we found that the aggressive phenotype was associated with altered expression of components of the Notch pathway, including Notch3, Delta-like 4 (DLL4), and Jagged-1 ligands. Stimulation with immobilized recombinant DLL4 or transduction with DLL4-expressing vectors dramatically increased Notch3 expression in CRC cells, associated with accelerated tumour growth. Forced expression of an active form of Notch3 mirrored the effects of DLL4 stimulation and increased tumour formation. Conversely, attenuation of Notch3 levels by shRNA resulted in perturbation of the cell cycle followed by reduction in cell proliferation, clonogenic capacity, and inhibition of tumour growth. Altogether, these findings indicate that Notch3 can modulate the tumourigenic properties of CRC cells and contributes to sustained Notch activity in DLL4-expressing tumours.

Keywords: Notch3; DLL4; angiogenesis; colorectal cancer

Received 10 February 2010; Revised 2 March 2010; Accepted 4 March 2010

No conflicts of interest were declared.

Introduction

Notch genes encode transmembrane receptors that are strictly required for normal embryonic development and regulate differentiation and survival of stem and/or progenitor cells in a variety of tissues [1–3]. Four Notch proteins have been described (Notch1, 2, 3, and 4) that serve as receptors for the Delta-like (DLL1, DLL3, and DLL4) and Jagged (Jagged-1 and Jagged-2) ligands [4]. According to the canonical model of Notch activation, ligand binding leads to two subsequent proteolytic cleavages that release the Notch intracellular domain (Notch-ICD). The Notch-ICD then translocates into the nucleus, where it interacts with CSL transcription factors to form a complex which activates the expression of genes suppressed in the absence of a Notch signal [5–7]. A link between abnormalities of the Notch pathway and human cancer has been identified in T-cell acute lymphoblastic leukaemias (T-ALLs), in which activating mutations of the *Notch1* gene have been found in more than 50% of cases [8–10]. In addition to Notch1, deregulated Notch3 signalling has been proposed to be important in T-ALL, in view of the oncogenic potential of the Notch3 ICD in transgenic mouse models [11].

Moreover, altered Notch signalling has been observed in different solid tumours, including clear cell renal carcinoma, ovarian cancer, melanoma, glioma,

breast cancer, pancreatic and lung cancer, medulloblastoma, cervical carcinomas, and colorectal cancer (CRC) (reviewed in ref 12). Interestingly, Notch3 is amplified in 20% of ovarian cancers [13] and it is overexpressed in about 40% of non-small cell lung cancers [14]. Notably, Notch3 suppression results in loss of the transformed phenotype, indicating that this receptor contributes to Notch signalling in these malignancies. Since Notch mutations in solid tumours are rare, with the possible exception of lung cancer [15], other mechanisms of activation, including Notch gene amplification [13], loss of negative regulators (such as NUMB) [16], and activation by ligands [17,18] or loops involving certain cytokines (such as IL-6) [19], have been proposed.

In normal gut, both Notch1 and Notch2 signalling are implicated in the control of cell differentiation [20,21]. In this context, Notch activation leads to HES-1 up-regulation and down-regulation of *ATOH1* (gene) involved in the differentiation of precursors towards goblet cells [22]. Expansion of the crypt compartment accompanied by the inhibition of cellular differentiation and apoptosis are among the earliest signs of tumourigenesis in the colon [23]. Because Notch signalling inhibits terminal differentiation of goblet cells, aberrant Notch activation could be involved in the pathogenesis of colorectal tumours [24,25]. Indeed, two recent reports have unravelled the cross-talk between Notch1 and the Wnt pathway in colon adenomas, through β-catenin-mediated transcriptional activation of the Notch ligand Jagged-1 [26,27]. Furthermore, several studies have shown that Notch1 and the Jagged-1 and DLL4 ligands are commonly expressed in CRC [25,28–30]. Whether other Notch receptors are involved in CRC has not been investigated so far.

Recently, we demonstrated that expression of the Notch ligand DLL4 in the angiogenic tumour microenvironment contributes to the regulation of Notch3 signalling in subcutaneous models of tumour dormancy [31]. This suggested the existence of cross-talk between tumour and endothelial cells (ECs) involving the Notch3–DLL4 interaction. Here, we report that Notch3 and DLL4 are broadly expressed in human CRC samples and that DLL4 strongly up-regulates Notch3, leading to perturbation of Notch receptor expression in CRC cells. Moreover, we show that regulation of Notch3 levels in xenograft models markedly contributes to modulate CRC cell proliferation and tumourigenic potential.

Materials and methods

Cell lines and *in vitro* culture

The MICOL-14 cell line was derived from a lymph node metastasis of rectal cancer [32] and is poorly tumourigenic following subcutaneous injection into NOD/SCID mice; a tumourigenic variant of MICOL-14 cells, termed MICOL-14^{tum}, was obtained as previously described [31]. MICOL-S, MICOL-29, CG-705, CG-756, and CG-758 cell lines were all derived from human CRC biopsies [32]. HT29 and LOVO cell lines were purchased from the American Type Culture Collection. All cell lines were grown in RPMI 1640 medium supplemented with 10% FCS and 1% L-glutamine (Invitrogen, Milan, Italy) and used within 6 months from thawing and resuscitation. To stimulate Notch signalling, P12 wells were coated with soluble recombinant human DLL4 (4 μg/ml) or Jagged-1 (8 μg/ml) (R&D, Minneapolis, MN, USA) in PBS–BSA 0.1%; 1 day later, MICOL-14 cells were added at a concentration of 4×10^4 cells per well in complete medium and cultivated for 72 h prior to subsequent analysis.

To measure proliferation, cells were plated in 96-well plates at a concentration of 3×10^3 cells per well, and proliferation was evaluated at various time points by the ATP-based ViaLight HS BioAssay kit (Lonza, Basel, Switzerland).

Patients and tissue samples

For transcriptome analysis, 20 patients who underwent surgery at the University Hospital of Erlangen for the first manifestation of CRC were included. Patients who underwent preoperative radiation or chemotherapy were not included in this study, nor were patients with familiar CRC or inflammatory bowel disease. Fresh snap-frozen biopsies were obtained from all patients and used for RNA extraction. Further patients' details are reported in the Supporting information, Supplementary Table 1 and elsewhere [33]. The whole microarray experiment design, setup, and results are available through ArrayExpress (http://www.ebi.ac.uk/arrayexpress/), using the access number E-MEXP-833.

For tissue microarray (TMA) studies, formalin-fixed and paraffin-embedded tissue blocks and corresponding pathology reports were obtained for 177 sequential patients with CRC undergoing surgery from 1997 to 2000 at the John Radcliffe Hospital, Oxford, UK. Further details on this series of samples are reported in the Supporting information, Supplementary Table 2 and elsewhere [28]. Approval for the use of all human tissues was obtained from the local research ethics committee.

Immunohistochemistry (IHC)

For immunohistochemical analysis, 5 μm-thick paraffin-embedded tumour sections were rehydrated and then antigen retrieval was performed by incubation with 0.01 M citrate buffer (pH 6.0) at 95 °C for 20 min. After saturation with 1.5% pre-immune serum, slides were incubated with rabbit anti-HES-1 (Millipore, Billerica, MA, USA), the mouse anti-human Notch3 1E4 antibody (Ab), generated against Notch3 extracellular domain [34], or an anti-activated Notch1 Ab (Ab8925; Abcam, Cambridge, UK), raised against the N-terminus of the Notch1 intracellular domain. For studies in xenografts, rabbit anti-DLL4 Ab reacting with both

human and mouse DLL4 (Ab7280; Abcam) was used. For IHC staining of human tumours, a monoclonal anti-DLL4 Ab binding to the extracellular domain of human DLL4 and generated in VelocImmune mice (Regeneron Pharmaceuticals, Inc, Tarrytoen, NY, USA) was used [28]. To investigate Jagged-1 expression, a goat anti-human Jagged-1 Ab (R&D) was used. Basal membrane was stained by a mouse anti-human collagen IV mAb (Clone CIV 22; Dako, Glostrup, Denmark). Cell proliferation was evaluated by staining with the anti-Ki67 antibody (Novocastra Laboratories, Newcastle, UK) or a rabbit anti-phospho-histone H3 Ab (Ser10; Cell Signaling, Danvers, MA, USA), according to the manufacturer's instructions.

The slides were subsequently washed and incubated with the appropriate secondary Ab. Immunostaining was performed using the avidin–biotin–peroxidase complex technique (Vectastain ABC kit; Vector Labs, Burlingame, CA, USA), and 3,3′-diaminobenzidine (DAB kit; Dako) was used as a chromogen substrate. Finally, tumour sections were counterstained with Mayer's haematoxylin. The specificity of each staining procedure was confirmed by replacing the primary Ab with PBS.

Tumourigenicity assay

NOD/SCID mice were purchased from Charles River (Wilmington, MA, USA). Procedures involving animals and their care conformed to institutional guidelines that comply with national and international laws and policies (EEC Council Directive 86/609, OJ L 358, 12 December 1987). For tumour establishment, exponentially growing MICOL-14 and MICOL-14^{tum} cells or their derivatives were washed and resuspended in PBS. Seven- to nine-week-old male mice were injected subcutaneously with 5×10^5 cells in a 200 µl total volume in both dorsolateral flanks. The resulting tumours were inspected weekly and measured by calibre; tumour volume was calculated by the following formula: tumour volume (mm^3) = $L \times l^2 \times 0.5$, where L is the longest diameter, l is the shortest diameter, and 0.5 is a constant to calculate the volume of an ellipsoid. At the end of the experiment, the mice were sacrificed by cervical dislocation; the tumours were harvested by dissection and either snap-frozen or fixed in formalin and embedded in paraffin for further analyses.

Statistical analysis

Results were expressed as mean value ± SD. Statistical analysis of the data was performed using Student's t-test. Differences were considered statistically significant when $p < 0.05$.

Statistical analysis of TMA data was carried out using PASW Statistics version 18.0 (SPSS Inc, Chicago, IL, USA). Correction for multiple hypothesis testing was performed using the false discovery rate controlling procedure [28].

Results

Notch3 is frequently expressed in human CRC samples and cell lines

Screening of a panel of eight human CRC cell lines, most of which derived from primary cultures [32], disclosed that Notch1–3 transcripts were expressed by all cell lines analysed, whereas Notch4 was detected only in HT29 cells (Figure 1A). To investigate Notch3 expression in primary tumour samples, the commercial Gene Logic database of Affymetrix HG-U133 GeneChip expression microarray data was queried for probe sets corresponding to Notch3. Details about this database may be found in the Supporting information, Supplementary materials and methods. The results indicated that Notch3 transcripts were significantly up-regulated in primary cancer and metastasis compared with matched normal mucosa, whereas they were significantly down-regulated in adenoma (Supporting information, Supplementary Figure 1). These findings were confirmed by the analysis of an independent set of microarray data obtained from 20 CRC samples, stages I–IV, and nine normal controls (Supporting information, Supplementary Table 1 and ref 33), indicating that Notch3 levels were significantly up-regulated in CRC versus normal mucosa, independently of stage (Figure 1B).

Based on these transcriptional data, we analysed Notch3 expression by IHC in a series of 158 CRC samples by using TMA. In normal colon mucosa, Notch3 was expressed rarely by some normal epithelial cells, generally with a weak intensity of staining, whereas it was expressed at strong/moderate levels by 19.7% of the CRCs analysed and at weak levels by 51.2% of the samples (Table 1). The pattern of Notch3 staining was cytoplasmic (Figure 1C), as previously reported by others [34]. In about one-third of the samples (29.1%), we could not detect Notch3 by IHC. As this antibody recognizes an epitope of the extracellular Notch3 domain, it is not possible to conclude whether strong expression correlates with increased Notch3 activation. Notch3 expression was not correlated with specific clinicopathological variables (Supporting information, Supplementary Table 3) or with prognosis of patients (Supporting information, Supplementary Table 4).

Since Notch3 protein was strongly expressed by about 20% of tumours and was still poorly characterized in this context, we focused on the mechanism of Notch3 up-regulation and its possible oncogenic role.

DLL4 and Jagged-1 are detected in CRC

To investigate the possibility that Notch activity might be regulated by Notch ligands, we analysed their expression in the tumour microenvironment. Jagged-1 was overexpressed in CRC samples compared with normal mucosa, and it was detected in both malignant epithelial cells and ECs (Figure 2A and Table 1). Among other Notch ligands, DLL4 expression was

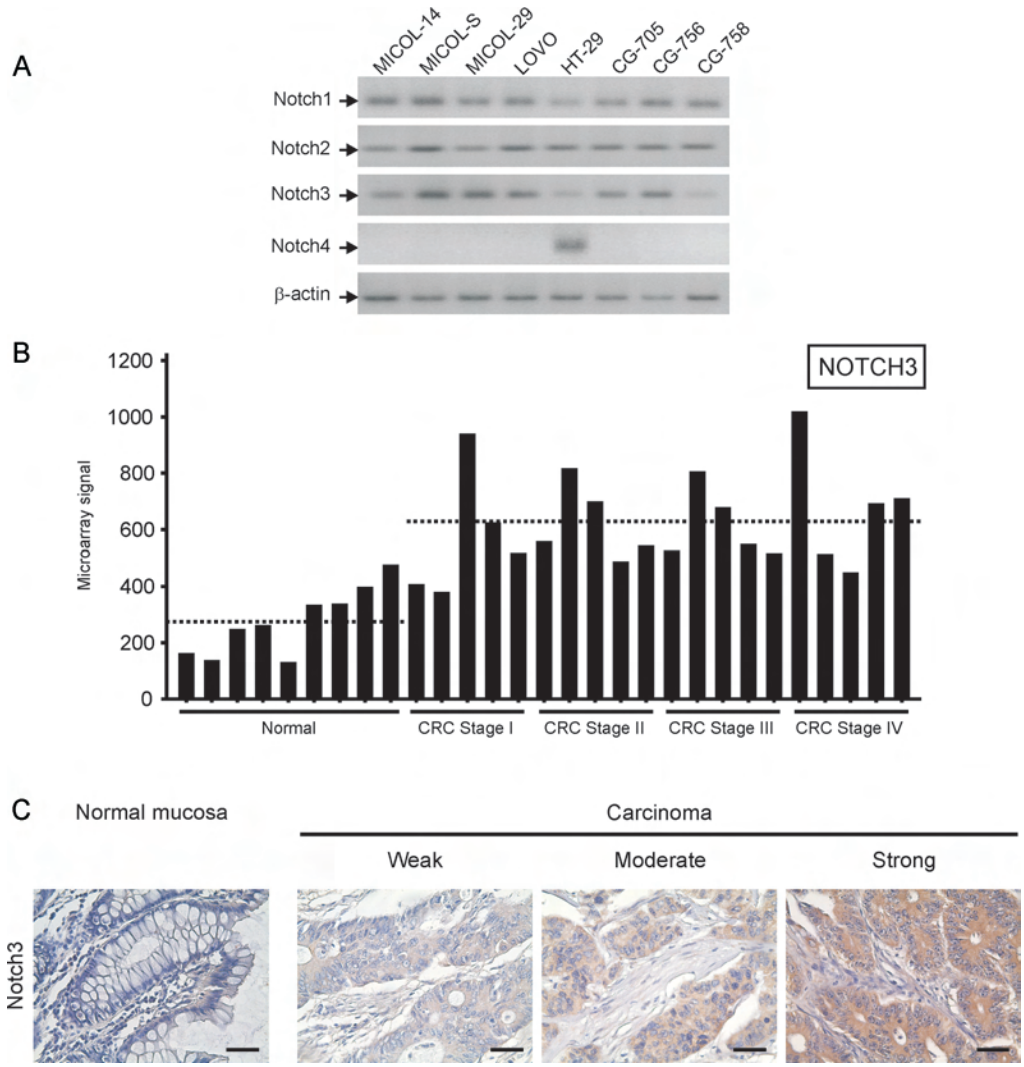

Figure 1. Notch3 is frequently expressed in human CRCs. (A) End-point RT-PCR analysis shows broad expression of Notch1–3 receptors in CRC cell lines. Notch4 was detected only in HT-29 cells. β-Actin was used to normalize samples. (B) Significant perturbations in *Notch3* RNA levels in CRCs versus normal colon mucosa by HG-U133A microarray analysis ($p < 0.05$, Mann-Whitney *U*-test). Columns: intensity of probe expression in individual samples; dotted lines: median value for each group of samples. (C) Notch3 expression in CRCs by IHC. Panels show representative samples with different intensities of staining along with normal colon mucosa. The anti-human Notch3 1E4 Ab was used [34]. Original magnification ×400**.**

Table 1. Results of IHC staining of CRC TMA

	Activated Notch1		Notch3		DLL4		Jagged-1	
	Frequency	%	Frequency	%	Frequency	%	Frequency	%
Tumour	Cytoplasm*						Cytoplasm*	
0	15	4.8	46	29.1	150	85.7	68	39.3
1	29	18.2	81	51.2	25	14.3	45	26.0
2	65	50.3	28	17.8			59	34.1
3	38	26.7	3	1.9			1	0.6
Total	147	100.0	158	100.0	175	100.0	173	100.0
	Nuclear*						Nuclear*	
0	126	85.7					93	53.8
1	21	14.3					80	46.2
Total	147	100					173	100.0
Vessels								
0	69	41.8	146	92.4	50	28.6	150	86.7
1	96	58.2	12	7.6	125	71.4	23	13.3
Total	165	100.0	158	100.0	175	100.0	173	100.0

*Jagged-1 and Notch1 staining yielded both cytoplasm and nuclear signals, which were scored separately.

Notch3 and DLL4 stained exclusively the cytoplasm of positive cells.

Evaluation of tumour cytoplasmic staining: 0, negative; 1, weak; 2, moderate; 3, strong. Nuclear staining: 0, absent; 1, present. Vessel staining: 0, absent; 1, present.

Core attrition in tissue microarrays is responsible for missing cases.

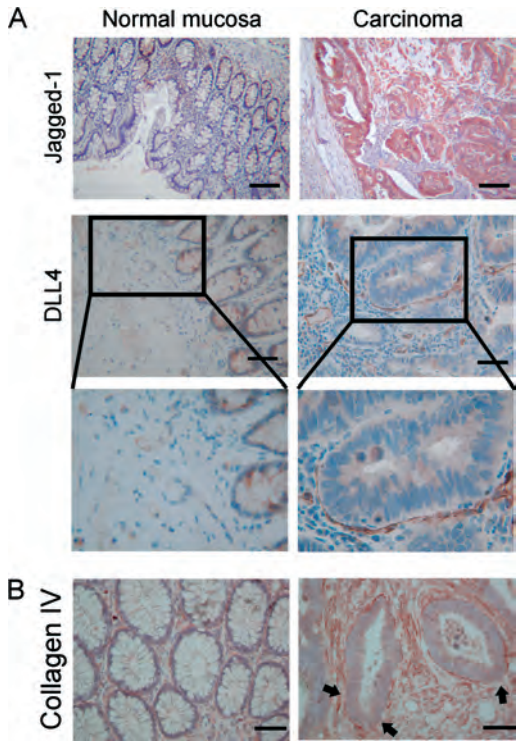

Figure 2. Expression of the Notch ligands Jagged-1 and DLL4 in CRC. (A) Panels show representative CRC samples along with normal colon mucosa. Original magnification ×200; the boxed areas are magnified (original magnification ×400) to show the proximity between DLL4^{+} ECs and cancer cells. (B) Staining of the basal membrane in tumours or normal mucosa. The basement membrane surrounding epithelial cells, decorated by an anti-human collagen IV mAb, is discontinuous in the tumour sample, whereas it is continuous in the normal mucosa. Original magnification ×250.

investigated by using an Ab specific to human DLL4 recently validated in another study [28]. In normal colon mucosa, DLL4 staining was weak and limited to 10–20% of small vessels; in cancer, however, DLL4 was brightly expressed by almost all blood vessels present in the section (Figure 2A and Table 1). Moreover, the spatial distribution of DLL4^{+} vessels differed between the two conditions. In normal colon, sporadic DLL4^{+} endothelial cells (ECs) were resident in the sub-mucosa, whereas in tumours, DLL4^{+} vessels penetrated into the tumour mass and were often contiguous to malignant epithelial cells, thus allowing possible cell–cell interactions (Figure 2A, boxed area), also facilitated by discontinuity of the basal membrane in tumours, as opposed to normal mucosa (Figure 2B). Other cell types of the stroma, such as fibroblasts, lacked DLL4 expression, in line with previous observations [28].

Intriguingly, a positive association between DLL4 expression in blood vessels and Notch3 expression at moderate/high levels in tumour cells was noted ($\chi^2 = 8.65$; $p = 0.034$). Moreover, although Notch3 expression in tumour cells did not correlate with Jagged-1 expression in EC ($\chi^2 = 1.06$; $p = 0.86$), it correlated with cytoplasmic Jagged-1 levels in tumour cells ($\chi^2 = 25.26$; $p = 0.003$). Altogether, these results suggest that DLL4 and Jagged-1 ligands could contribute to sustain Notch3 expression in CRC.

Up-regulation of Notch3 is a feature of aggressive CRC xenografts

To further investigate the possibility that signals stemming from the ligands might regulate Notch activity in tumour cells, we exploited a xenograft model recently established in our laboratory by using human CRC cells with different tumourigenic capacities in NOD/SCID mice. As previously observed [31], MICOL-14 cells behaved as dormant when injected into the subcutaneous tissue of the mice, whereas the variant termed MICOL-14^{tum} was able to generate large vascularized tumours by 6 weeks from injection (Supporting information, Supplementary Figure 2A). This may in part depend on the higher angiogenic potential of MICOL-14^{tum} compared with MICOL-14 cells, as shown by the results of the CAM assay performed with conditioned medium from the cells (Supporting information, Supplementary Figure 2B). In agreement with this, the numbers of Ki67^{+} proliferating cells were significantly higher in aggressive than in dormant tumours (Supporting information, Supplementary Figure 2C). Apoptosis levels were low and comparable in both tumour entities (not shown).

Expression of several components of the Notch pathway, including Notch1, Notch3, HES-1, and HEY-2, was markedly increased in MICOL14^{tum}-derived tumour RNA compared with dormant tumours (Supplementary table V and Figure 3A, top), suggesting that Notch activation is a feature of aggressive xenografts. This was also indicated by the detection of higher Notch3 ICD levels in aggressive compared with dormant tumours (Figure 3A, middle and bottom). The latter samples also had detectable, albeit low, Notch3 ICD levels, possibly due to activation of Notch3 by Jagged-1 which is expressed by MICOL14 cells (not shown), or other Notch ligands not scored here. Notably, however, Notch3 transcript and ICD levels were similar in MICOL-14^{tum} and MICOL-14 cells grown *in vitro*, as it was Notch activity determined by a Notch-responsive luciferase reporter assay (Supporting information, Supplementary Figure 3), indicating that increased Notch activation is not a cell-autonomous event.

IHC confirmed the qPCR results showing higher expression of HES-1, DLL4, and Jagged-1 in aggressive compared with dormant tumours (Figure 3B). Abundant expression of Jagged-1 and HES-1 was found in tumour cells, whereas DLL4 was mainly expressed by stromal cells, including both ECs and cells with fibroblast morphology (Figure 3B).

The observation that deregulation of the Notch pathway is associated with strikingly different kinetics of tumour growth convinced us to exploit the MICOL14/MICOL14^{tum} model to further investigate how Notch3 expression and activity are regulated.

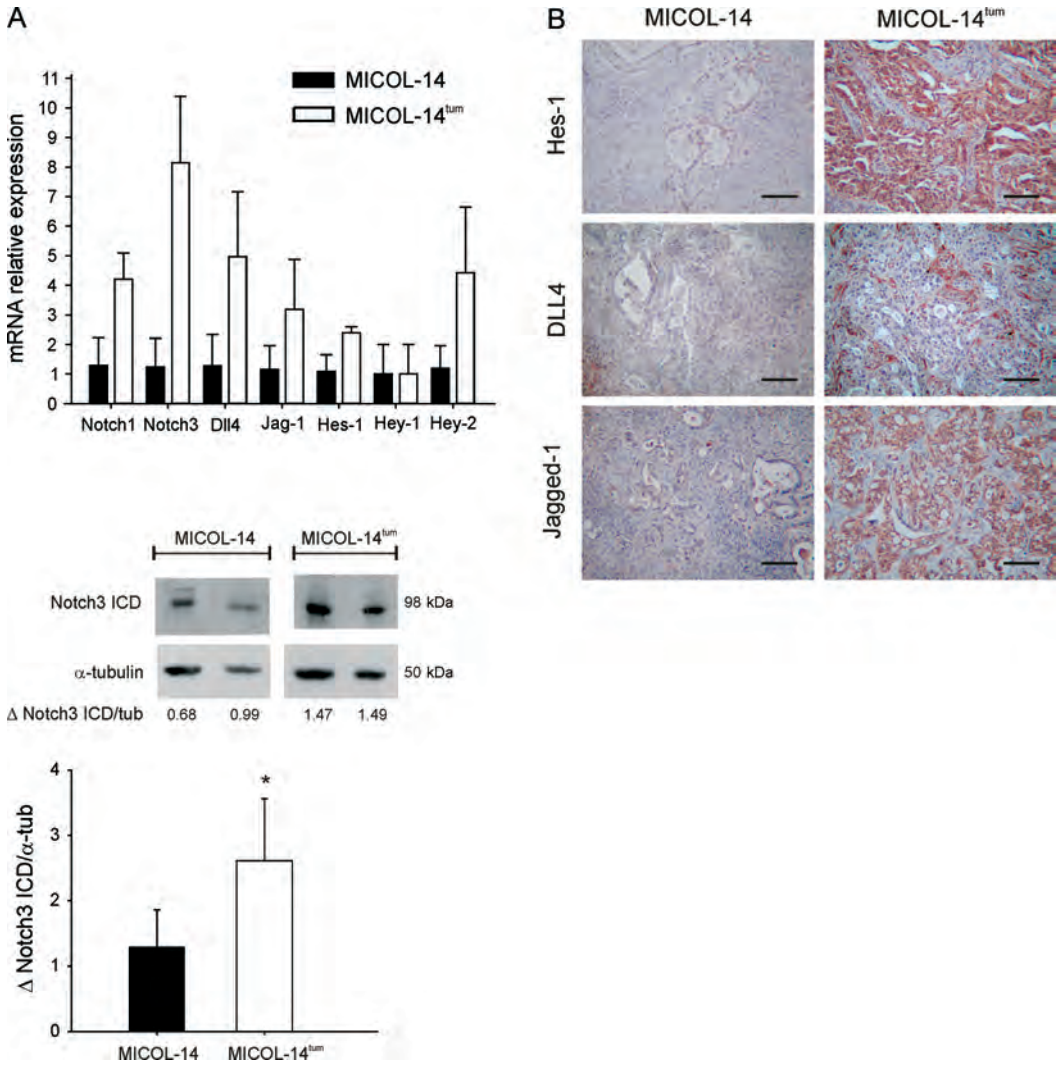

Figure 3. Deregulation of the Notch pathway in a model of CRC cell dormancy. (A) Upper panel: Notch1 and Notch3 transcripts, along with certain Notch target genes (HES-1, HEY-1, HEY-2) and ligands (DLL4, Jagged-1), are highly expressed in aggressive tumours by real-time PCR. Columns: means of duplicate determinations in four samples; bars: SD; $^{*}p < 0.05$. Middle panel: the left panel shows variations in Notch3 ICD levels in aggressive compared with dormant MICOL-14 tumours. Two representative samples per group are shown. α-Tubulin was used for normalization. Bottom panel: columns report the mean values ± SD of Notch3 ICD/α-tubulin ratios in all samples analysed ($n = 4–8$ per group). (B) HES-1, DLL4, and Jagged-1 expression in xenografts of MICOL-14 cells. Original magnification ×200.

DLL4 stimulation induces Notch3 expression and promotes tumour growth

Since MICOL-14^{tum} xenografts and CRC samples expressed both Jagged-1 and DLL4, we sought to investigate the relative potency of these ligands in engaging Notch receptors in CRC cells. To this end, MICOL-14 cells were plated on either human DLL4- or Jagged-1-coated wells and the expression of Notch target genes was measured. Recombinant DLL4 (4 μg/ml) activated *HES-1* and *HEY-2* expression at the RNA level (Figure 4A, left panel). The effect of Jagged-1 was clearly lower, even at higher concentrations (8 μg/ml). In these experiments, we also observed a robust (12-fold) increase of *Notch3* mRNA following DLL4 stimulation of MICOL-14 cells, whereas *Notch1* levels remained substantially unperturbed (Figure 4A, left panel). Assessment of Notch signalling by a Notch luciferase reporter construct transiently transfected into MICOL-14 cells confirmed these findings (Figure 4A, right panel). Murine DLL4 had similar effects to human DLL4 on Notch activation (not shown). Further confirmation was obtained by IF and WB analysis, indicating increased Notch3 full-length and ICD levels in these cells following stimulation with DLL4 (Figure 4B). Since *Notch3* is a known transcriptional target of *Notch1* [35,36], these findings might reflect activation of Notch1 by DLL4. Indeed, we detected activated Notch1 in MICOL-14 cells by IFA (not shown), and attenuation of Notch1 expression by specific shRNA partly reduced DLL4-dependent up-regulation of Notch3 levels (Figure 4C), indicating that Notch1 may in part contribute to this phenomenon.

Moreover, by using an antibody that specifically recognizes the activated version of the Notch1 receptor [15], Notch1 was also detected in TMA, often with stronger reactivity compared with Notch3 (Table 1 and Supporting information, Supplementary Figure 4), and its expression in the cytoplasm of tumour cells

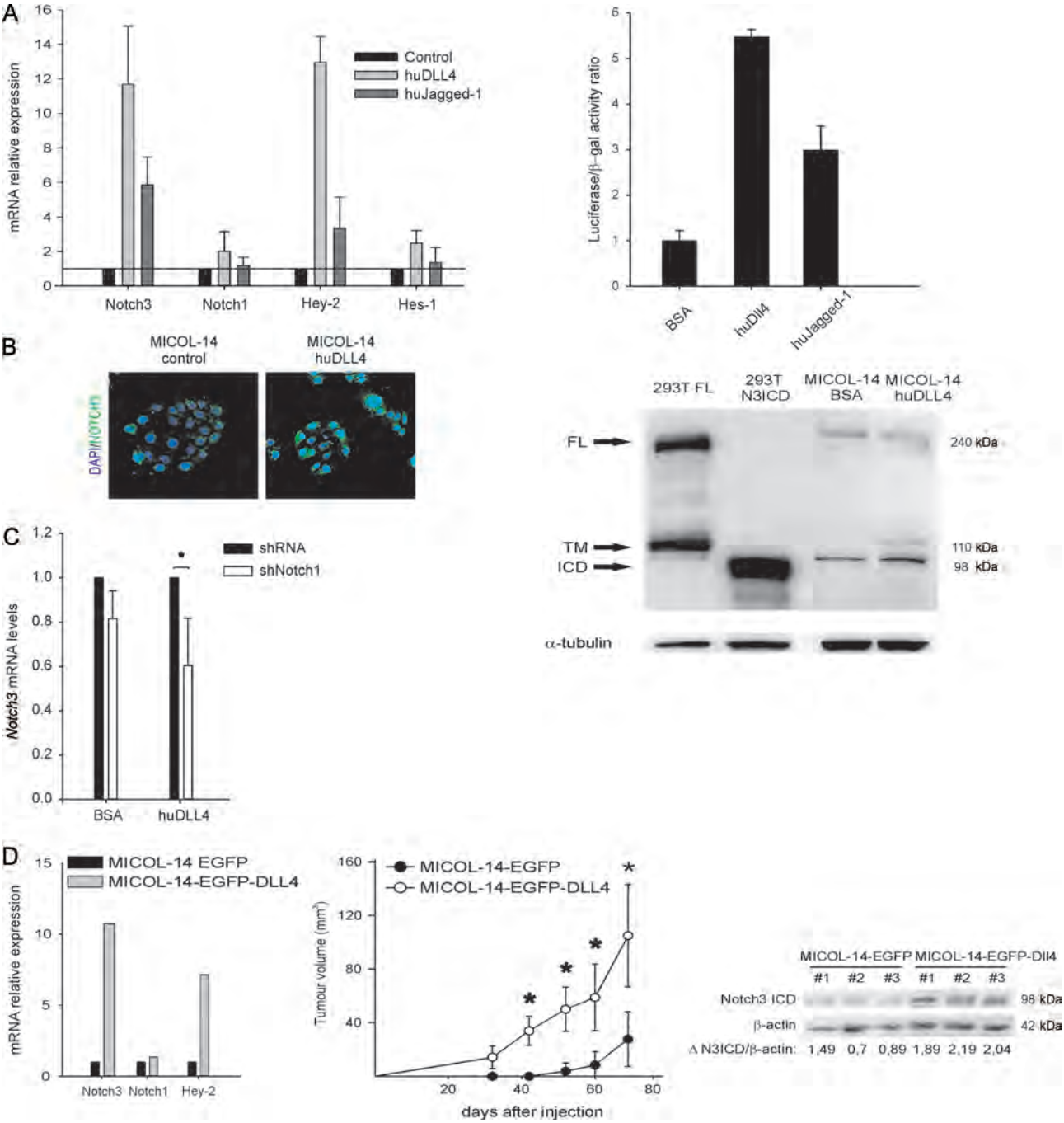

Figure 4. Stimulation by DLL4 up-regulates Notch3 expression in CRC cells and confers a tumourigenic phenotype. (A) Left panel: increased expression of *Notch3* and *HEY2* in MICOL-14 cells cultivated for 72 h on recombinant human DLL4 (4 μg/ml) or Jagged1 (8 μg/ml) by quantitative PCR analysis. Columns: mean values of three independent experiments; bars: SD. $^*p < 0.05$. Right panel: DLL4 and Jagged-1 increase Notch activity in MICOL-14 cells by a luciferase reporter assay. Experimental details are provided in the Supporting information, Supplementary materials and methods. The bars represent the mean ± SD of three independent experiments. (B) Increased Notch3 expression in MICOL-14 cells following incubation on DLL4-coated wells for 72 h by IFA using an Ab (M134, Santa Cruz Biotech) to the C-terminus of Notch3 (left panel) or western blot analysis with rabbit anti-Notch3 Ab (Ab23426, Abcam) (right panel). The bands corresponding to Notch3 full-length (FL), transmembrane Notch (TM), and ICD following transient transfection of 293T cells with plasmids encoding either Notch3 FL or ICD are indicated by the arrows; α-tubulin was used for normalization. (C) Induction of Notch3 transcripts by DLL4 stimulation is partially dependent on Notch1. MICOL-14 cells were transduced with either a Notch1 shRNA-encoding or a control vector (shRNA) and subsequently cultivated on DLL4-coated or control (BSA) wells for 4 days. Notch3 transcript levels were measured by quantitative PCR and normalized to those measured in control cells (shRNA). The bars represent the mean ± SD of three independent experiments. $^*p < 0.05$. (D) Left panel: transduction of the DLL4 cDNA leads to marked up-regulation of Notch3 and HEY-2 transcripts in MICOL-14 cells. One representative experiment of two performed is shown. Middle panel: tumour-promoting effects of forced DLL4 expression in MICOL-14 cells. The graph shows the kinetics of tumour growth following subcutaneous injection of MICOL-14 cells transduced by DLL4–EGFP or the control retrovirus in NOD/SCID mice ($n = 5$ mice per group). Right panel: evaluation of Notch3 ICD levels in tumour samples by western blotting. β-Actin was used for normalization.

correlated positively with endothelial DLL4 ($\chi^2 = 9.15$; $p = 0.027$) and tumour Notch3 ($\chi^2 = 27.27$; $p = 0.001$) expression. Notably, activated Notch1 was not a significant prognostic factor at multivariate analysis (data not shown). These results strengthen the hypothesis that Notch signalling in CRC is driven by a heterotypic interaction between DLL4-expressing endothelial cells and tumour cells expressing Notch receptors.

We then ectopically expressed DLL4 in MICOL-14 cells by using a previously described EGFP–DLL4-encoding retroviral vector [37]. Subsequent expression analyses showed that this strongly increased *Notch3* and *HEY-2* transcripts, with only minimal changes in Notch1 levels (Figure 4D, left panel). Importantly, forced expression of DLL4 dramatically increased the tumourigenic potential of dormant MICOL-14 cells (Figure 4D, middle panel), and this was associated with increased Notch3 ICD levels in tumours (Figure 4D, right panel). Altogether, these findings indicate that DLL4 strongly up-regulates Notch3 expression and this correlates with accelerated growth of CRC xenografts.

Notch3 silencing in CRC cells reduces proliferation and clonogenic capacity *in vitro* and impairs tumourigenicity *in vivo*

To establish the biological functions of Notch3 in CRC cells, we attenuated its expression by using lentiviral vectors encoding a specific shRNA. Following shRNA delivery, *Notch3* RNA levels were reduced by 60–80% compared with control MICOL-14^{tum} cells (Figure 5A). Notch3-silenced cells displayed a substantial reduction of target gene expression, including *HES-1* and *HEY-1* and -2 (Figure 5A). Similar results were obtained with a second CRC cell line, termed MICOL-S (Figure 5A).

Notch3 silencing was followed by a dramatic change in tumour cell morphology. As shown in Figure 5B, MICOL-14^{tum} and MICOL-S cells transduced by the shNotch3 vector displayed a spike-like shape compared with control cells, which maintained a more flattened phenotype. We also measured a moderate—albeit significant—decrease of cell proliferation following silencing of Notch3 (Figure 5C, left). Cell cycle analysis indicated accumulation of cells in the G0/G1 phase, with corresponding reductions in the S phase (Figure 5C, right). Moreover, anchorage-independent growth of MICOL-14^{tum} cells bearing reduced Notch3 levels was severely impaired (>90%) in semisolid medium (not shown). On the other hand, down-modulation of Notch3 did not affect apoptosis levels in MICOL-14^{tum} and MICOL-S cells (not shown). In accordance with these *in vitro* results, xenograft growth was greatly delayed by Notch3 silencing in MICOL-14^{tum} cells, according to both standard measurements of tumour size and optical imaging analysis (Figure 5D).

On the other hand, forced Notch3 expression obtained by transduction of Notch3ΔE—an active form of human Notch3 [35]—into dormant MICOL-14 cells increased Notch3 and HEY-2 expression (Figure 6A) and accelerated tumour growth (Figures 6B and 6C). In these experiments, Notch1 and DLL4 transcript levels remained relatively unperturbed following transduction by the Notch3ΔE vector (Figure 6A). Proliferation was higher in tumours formed by cells overexpressing Notch3 (Figure 6D), indicating that deregulation of Notch3 signalling confers a proliferative advantage to MICOL-14 cells. Altogether, these findings indicate that Notch3 levels are crucial to determine the kinetics of subcutaneous growth of MICOL-14 xenografts.

Discussion

We have shown that Notch3 is expressed by about 70% of CRC samples and that DLL4 contributes to its up-regulation. DLL4 is frequently expressed by the stroma of CRC and its expression levels correlate with VEGF [28]. DLL4 was found to be expressed by tumour-associated ECs, which often established close contacts with cancer cells (Figure 2). In clinical samples, we observed a positive correlation between DLL4 and Notch3 expression in tumour cells. These findings suggest that DLL4 contributes to regulate Notch activity in CRC by heterotypic cell interactions, as recently shown in pre-clinical models of T-ALL [31]. Importantly, they expand recent findings obtained in mouse models of colon cancer, indicating that Notch signalling is triggered by ligands expressed on adjoining blood vessels and contributes to tumour invasion and intravasation [38].

A notable finding was the dramatic up-modulation of the Notch3 transcript and protein levels in CRC cells following stimulation by the DLL4 ligand or transfer of the *DLL4* gene. This result could reflect primary activation of Notch1, as Notch3 was previously identified as a Notch1 target gene in microarray studies [35,36]; indeed, reduction of Notch1 levels by specific shRNA partially blocked up-modulation of the Notch3 transcript by DLL4 (Figure 4C). Overall, the *in vitro* findings agree with the results of TMA studies, which showed a significant positive association between activated Notch1 and Notch3. Discordant samples, which express either Notch1 or Notch3, might underscore the existence of receptor-specific mechanisms of regulation of Notch expression, such as microRNA [39], or could be related to the different performances of the primary antibodies. In this respect, although it is known that colon adenomas have increased Notch signalling [26], Notch3 expression was surprisingly low in adenomas (Supporting information, Supplementary Figure 1), underscoring that *in vivo* complex interactions regulate the expression levels of Notch receptors.

Although in this study we focused on regulation of Notch3 expression and activity by DLL4, it is important to be aware of alternative explanations for our findings. With regard to the mechanisms causing

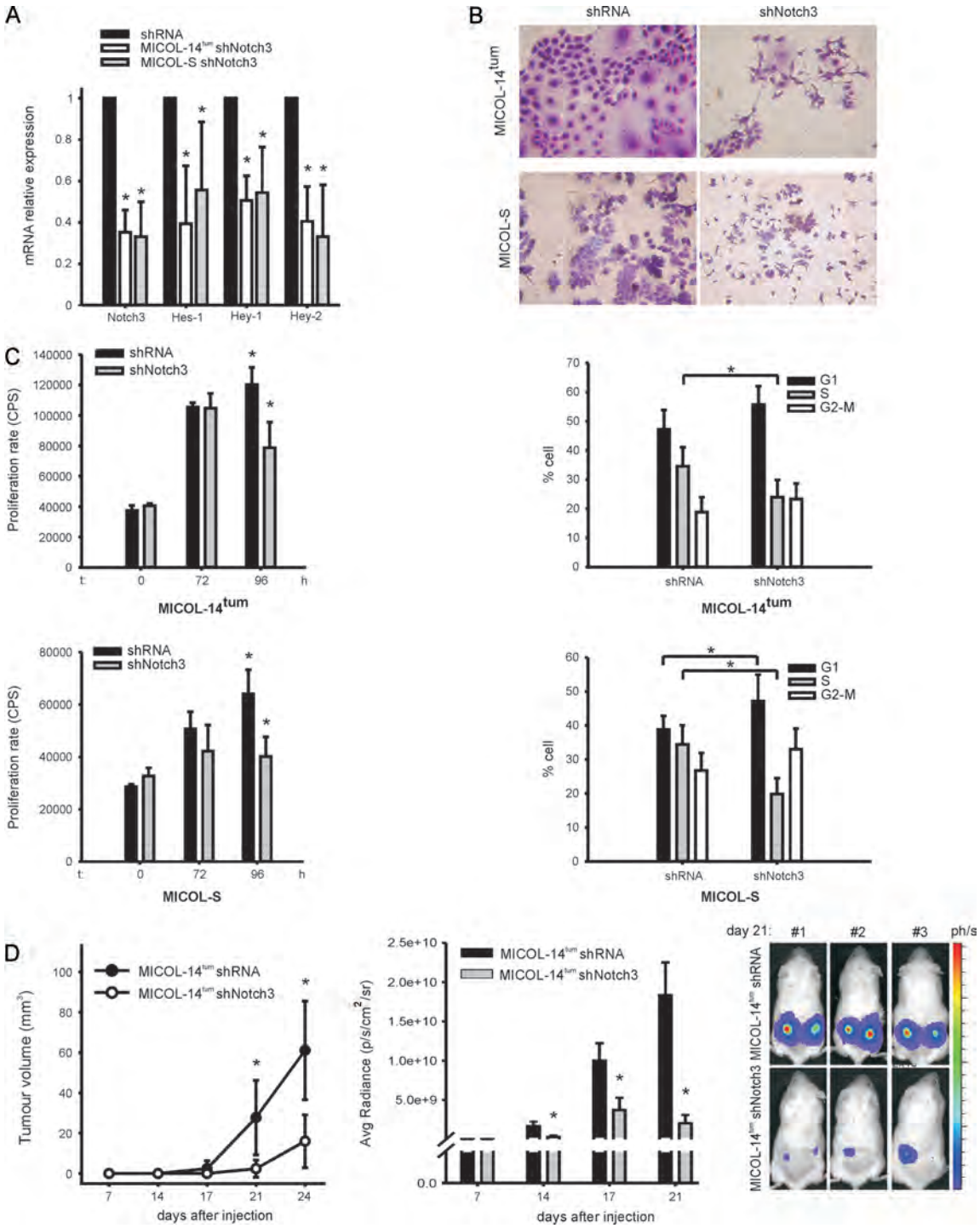

Figure 5. Attenuation of Notch3 levels impairs the proliferation of CRC cells and alters their tumourigenic capacity. (A) Reduced expression of Notch3 and Notch target genes in MICOL-14^{tum} and MICOL-S cells transduced by a lentiviral vector encoding a Notch3-specific shRNA (shNotch3) or a control vector (shRNA) by quantitative PCR analysis. Columns: mean values of three independent experiments performed in duplicate; bars: SD. $^*p < 0.05$. (B) Crystal violet staining of MICOL-14^{tum} and MICOL-S cells following Notch3 silencing. Notch3 inhibition led to cytoplasm shrinkage and alterations in cell size and shape. Original magnification $\times 20$. (C) Left panels: proliferation analysis of Notch3 or mock shRNA-transduced cell lines. Notch3 silencing causes a moderate, yet significant reduction of cell proliferation both in MICOL-14^{tum} and in MICOL-S cells 96 h after gene transfer. CPS = counts per second. Columns: mean values of three independent experiments; bars: SD. $^*p < 0.05$. Right panels: effects of Notch inhibition on the cell cycle profile of CRC cells. MICOL-14^{tum} and MICOL-S cells were treated with Notch3 shRNA or control vector (shRNA) for 5 days followed by propidium iodide staining and cell cycle analysis. Columns: mean values of three independent experiments; bars: SD. $^*p < 0.05$. (D) Effects of Notch3 inhibition on tumour growth. Left panel, kinetics of tumour growth following subcutaneous injection of MICOL-14^{tum} cells transduced by Notch3-specific or control shRNA in NOD/SCID mice ($n = 5$ mice per group). Middle and right panels: evaluation of tumour growth by imaging techniques following injection of luciferase-expressing MICOL-14^{tum} cells.

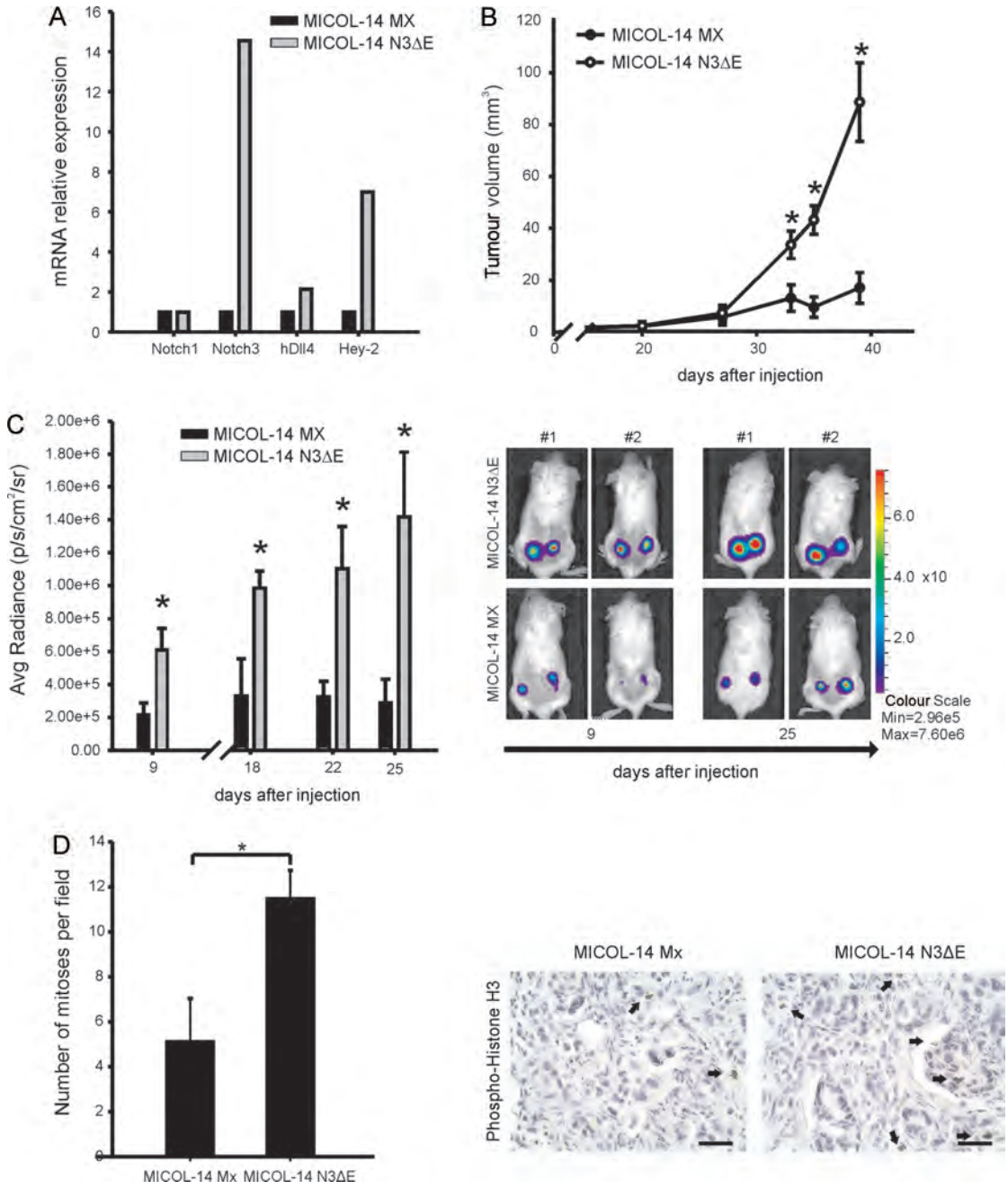

Figure 6. Up-modulation of Notch3 increases cell proliferation and the kinetics of tumour growth. (A) Measurement of transcript levels of components of the Notch pathway in MICOL-14 cells, following transduction by a retroviral vector encoding either a ligand-independent active form of Notch3 (N3ΔE) or a control vector (MX). Both vectors carry the *EGFP* gene to allow determination of the efficiency of gene transfer, which was 10% and 12% for N3ΔE- and MX-transduced cells, respectively. Quantitative PCR analysis was performed 4 days after transduction. One representative experiment out of three performed is shown. (B) Kinetics of tumour growth following subcutaneous injection of MICOL-14 cells transduced by N3ΔE or control vector (MX) in NOD/SCID mice ($n = 5$ mice per group). (C) Effects of Notch3 overexpression on tumour growth by imaging techniques, following injection of luciferase-expressing MICOL-14 cells. (D) Effects of Notch3 overexpression on cell proliferation *in vivo*. Columns indicate the mean ± SD values of phosphor-histone 3 (pH3) positive cells in $n = 5–6$ samples of each experimental group. $^*p < 0.05$. The right panels show representative images of pH3$^+$ cells in tumours (arrows). Original magnification ×200.

Notch3 overexpression and activation in CRC, to the best of our knowledge, mutations of Notch pathway components in CRC samples have rarely been reported [25,40]. Among other genetic mechanisms, *Notch3* gene amplification has been reported in ovarian cancer [13], and we are currently evaluating whether *Notch3* gene copy number is increased in cancer compared with normal colon mucosa.

Finally, the contribution of other ligands cannot be excluded. Although this aspect was not the main purpose of our study, we found increased expression of Jagged-1 in xenografts and CRC samples. These results substantially agree with previous studies which have shown increased expression of Jagged-1 either in colon adenomas [26,27] or in cancer [29]. In mice studies, Jagged-1—whose expression is in part controlled

by the WNT/β-catenin pathway—was considered the main driver of Notch1 activation in colon adenomas [27], and we also found that Jagged-1 activates Notch signalling in CRC cells. In this respect, the results of TMA studies indicate that Jagged-1 expressed by the tumour rather than stromal cells is correlated with Notch3 expression levels.

Previously, it was reported that Notch3 represses Notch1-mediated activation through HES promoters [41], suggesting that Notch3 could be a negative regulator of Notch1 signalling. In that study, the Notch3 ICD interfered with Notch1-mediated activation of HES-1 by competing with the Notch1 ICD for access to RBP-Jk and also by competing for a common co-activator. These data, however, could be cell-type or context-specific, as other groups have subsequently reported strong activation of HES-1 by activated Notch3 in CHO cells *in vitro* [42] or in Notch3 transgenic mice [11].

Our results support the hypothesis that Notch3 is transcriptionally active, as specific modulation of Notch3 levels regulated Notch signalling accordingly in CRC cells without substantial changes in Notch1 levels (Figure 6A). Moreover, forced expression of the active form of Notch3 increased the kinetics of growth of MICOL-14 xenografts. One mechanism could involve cell proliferation (Figure 6D), fitting with recent results of Notch1 up-regulation in CRC cells [30]. Conversely, attenuation of Notch3 levels reduced cell proliferation and the clonogenic potential of CRC cells. These effects are in line with those reported by other groups following genetic inactivation of Notch3 in breast, ovarian, and lung cancer cells [13,14,43], and they may reasonably explain why silencing Notch3 weakens the tumourigenic capacity of MICOL-14^{tum} cells and induces tumour dormancy. It should be stressed that genetic inactivation of Notch1 in CRC cells [30] or treatment with GSI [44] does not allow us to examine the possible contribution of Notch3 to the biological effects observed, as these interventions would simultaneously blunt the expression levels and activity of both receptors.

In conclusion, since Notch3 is downstream of DLL4 and it regulates key tumourigenic properties of CRC cells independently of Notch1, our results provide grounds for the future development of Notch3-targeted therapies. Finally, these data highlight the importance of stromal–tumour cell interaction in the framework of a major tumourigenic signal tranduction pathway in CRC.

Acknowledgment

We are indebted to the following colleagues for providing essential reagents: C Castelli and P Dalerba (Istituto Nazionale Tumori, Milan, Italy) for providing the CRC cell lines; K Vanderkerken (Vrije Universiteit Brussel, Belgium) for the firefly luciferase lentiviral vector; N Chadwick (University of Manchester, UK) for the MX and N3ΔE retroviral vectors; A Joutel (INSERM U749, France) for the full-length Notch3 plasmid and the 1E4 anti-human Notch3 Ab; M Bonafè (University of Bologna, Italy) for the Notch3 ICD plasmid; and H Turley (WIMM, Oxford, UK) for technical help with DLL4 IHC. We also wish to thank P Dalerba (Stanford University, Palo Alto, CA, USA) and R Fodde (Erasmus University Medical Center, Rotterdam, The Netherlands) for critical reading of the manuscript. AM Jubb is the recipient of a Career Development Fellowship from the Pathological Society of Great Britain and Ireland. This work was supported in part by grants from AIRC, FIRC; Ministry of University and Research, 60% and PRIN; Ministry of Health, Oncology Program 2006 (AA); Fondazione Cassa di Risparmio di Padova e Rovigo; and Banco Popolare di Verona (SI). MS, EN, and RSC were supported by grants from the Interdisciplinary Center for Clinical Research (IZKF) of the University of Erlangen-Nuremberg and the German Ministry of Education and Research (BMBF, 01E50807); ALH was supported by a grant from the Oxford NIHR Biomedical Research Programme.

Author contribution statement

VS, LP, LM, MG, MC, LB, MM, DR, and EN carried out the experiments. VS, GE, DR, MS, RSC, AMJ, ALH, and HK analysed and interpreted data. AA and SI were responsible for the study design and wrote the paper. All authors were involved in editing the paper and had final approval of the submitted and published versions.

References

Note: References 45–50 are cited in the Supporting information to this article.

1. Artavanis-Tsakonas S, Rand MD, Lake RJ. Notch signaling: cell fate control and signal integration in development. *Science* 1999; **284**: 770–776.
2. Chiba S. Notch signaling in stem cell systems. *Stem Cells* 2006; **24**: 2437–2447.
3. Gridley T. Notch signaling in vertebrate development and disease. *Mol Cell Neurosci* 1997; **9**: 103–108.
4. D'Souza B, Miyamoto A, Weinmaster G. The many facets of Notch ligands. *Oncogene* 2008; **27**: 5148–5167.
5. Hsieh JJ, Henkel T, Salmon P, *et al*. Truncated mammalian Notch1 activates CBF1/RBPJk-repressed genes by a mechanism resembling that of Epstein–Barr virus EBNA2. *Mol Cell Biol* 1996; **16**: 952–959.
6. Johnston SH, Rauskolb C, Wilson R, *et al*. A family of mammalian *Fringe* genes implicated in boundary determination and the *Notch* pathway. *Development* 1997; **124**: 2245–2254.
7. Kopan R. Notch: a membrane-bound transcription factor. *J Cell Sci* 2002; **115**: 1095–1097.
8. Ellisen LW, Bird J, West DC, *et al*. *TAN*-1, the human homolog of the *Drosophila Notch* gene, is broken by chromosomal translocations in T lymphoblastic neoplasms. *Cell* 1991; **66**: 649–661.
9. Lee SY, Kumano K, Masuda S, *et al*. Mutations of the *Notch1* gene in T-cell acute lymphoblastic leukemia: analysis in adults and children. *Leukemia* 2005; **19**: 1841–1843.

10. Weng AP, Ferrando AA, Lee W, *et al*. Activating mutations of *NOTCH1* in human T cell acute lymphoblastic leukemia. *Science* 2004; **306**: 269–271.
11. Bellavia D, Campese AF, Alesse E, *et al*. Constitutive activation of NF-kappaB and T-cell leukemia/lymphoma in Notch3 transgenic mice. *EMBO J* 2000; **19**: 3337–3348.
12. Miele L, Golde T, Osborne B. Notch signaling in cancer. *Curr Mol Med* 2006; **6**: 905–918.
13. Park JT, Li M, Nakayama K, *et al*. *Notch3* gene amplification in ovarian cancer. *Cancer Res* 2006; **66**: 6312–6318.
14. Haruki N, Kawaguchi KS, Eichenberger S, *et al*. Dominant-negative Notch3 receptor inhibits mitogen-activated protein kinase pathway and the growth of human lung cancers. *Cancer Res* 2005; **65**: 3555–3561.
15. Westhoff B, Colaluca IN, D'Ario G, *et al*. Alterations of the Notch pathway in lung cancer. *Proc Natl Acad Sci U S A* 2009; **106**: 22293–22298.
16. Pece S, Serresi M, Santolini E, *et al*. Loss of negative regulation by Numb over Notch is relevant to human breast carcinogenesis. *J Cell Biol* 2004; **167**: 215–221.
17. Choi JH, Park JT, Davidson B, *et al*. Jagged-1 and Notch3 juxtacrine loop regulates ovarian tumor growth and adhesion. *Cancer Res* 2008; **68**: 5716–5723.
18. Sjolund J, Johansson M, Manna S, *et al*. Suppression of renal cell carcinoma growth by inhibition of Notch signaling *in vitro* and *in vivo*. *J Clin Invest* 2008; **118**: 217–228.
19. Sansone P, Storci G, Tavolari S, *et al*. IL-6 triggers malignant features in mammospheres from human ductal breast carcinoma and normal mammary gland. *J Clin Invest* 2007; **117**: 3988–4002.
20. Riccio O, van Gijn ME, Bezdek AC, *et al*. Loss of intestinal crypt progenitor cells owing to inactivation of both Notch1 and Notch2 is accompanied by derepression of CDK inhibitors p27Kip1 and p57Kip2. *EMBO Rep* 2008; **9**: 377–383.
21. van Es JH, van Gijn ME, Riccio O, *et al*. Notch/gamma-secretase inhibition turns proliferative cells in intestinal crypts and adenomas into goblet cells. *Nature* 2005; **435**: 959–963.
22. Leow CC, Romero MS, Ross S, *et al*. Hath1, down-regulated in colon adenocarcinomas, inhibits proliferation and tumorigenesis of colon cancer cells. *Cancer Res* 2004; **64**: 6050–6057.
23. Augenlicht L, Velcich A, Mariadason J, *et al*. Colonic cell proliferation, differentiation, and apoptosis. *Adv Exp Med Biol* 1999; **470**: 15–22.
24. Katoh M, Katoh M. Notch signaling in gastrointestinal tract. *Int J Oncol* 2007; **30**: 247–251.
25. Qiao L, Wong BC. Role of Notch signaling in colorectal cancer. *Carcinogenesis* 2009; **30**: 1979–1986.
26. Fre S, Pallavi SK, Huyghe M, *et al*. Notch and Wnt signals cooperatively control cell proliferation and tumorigenesis in the intestine. *Proc Natl Acad Sci U S A* 2009; **106**: 6309–6314.
27. Rodilla V, Villanueva A, Obrador-Hevia A, *et al*. Jagged1 is the pathological link between Wnt and Notch pathways in colorectal cancer. *Proc Natl Acad Sci U S A* 2009; **106**: 6315–6320.
28. Jubb AM, Turley H, Moeller HC, *et al*. Expression of delta-like ligand 4 (Dll4) and markers of hypoxia in colon cancer. *Br J Cancer* 2009; **101**: 1749–1757.
29. Reedijk M, Odorcic S, Zhang H, *et al*. Activation of Notch signaling in human colon adenocarcinoma. *Int J Oncol* 2008; **33**: 1223–1229.
30. Zhang Y, Li B, Ji ZZ, *et al*. Notch1 regulates the growth of human colon cancers. *Cancer* 2010; **116**: 5207–5218.
31. Indraccolo S, Minuzzo S, Masiero M, *et al*. Cross-talk between tumor and endothelial cells involving the Notch3–Dll4 interaction marks escape from tumor dormancy. *Cancer Res* 2009; **69**: 1314–1323.
32. Dalerba P, Guiducci C, Poliani PL, *et al*. Reconstitution of human telomerase reverse transcriptase expression rescues colorectal carcinoma cells from *in vitro* senescence: evidence against immortality as a constitutive trait of tumor cells. *Cancer Res* 2005; **65**: 2321–2329.
33. Naschberger E, Croner RS, Merkel S, *et al*. Angiostatic immune reaction in colorectal carcinoma: impact on survival and perspectives for antiangiogenic therapy. *Int J Cancer* 2008; **123**: 2120–2129.
34. Joutel A, Andreux F, Gaulis S, *et al*. The ectodomain of the Notch3 receptor accumulates within the cerebrovasculature of CADASIL patients. *J Clin Invest* 2000; **105**: 597–605.
35. Chadwick N, Zeef L, Portillo V, *et al*. Identification of novel Notch target genes in T cell leukaemia. *Mol Cancer* 2009; **8**: 35.
36. Palomero T, Lim WK, Odom DT, *et al*. NOTCH1 directly regulates c-MYC and activates a feed-forward-loop transcriptional network promoting leukemic cell growth. *Proc Natl Acad Sci U S A* 2006; **103**: 18261–18266.
37. Williams CK, Li JL, Murga M, *et al*. Up-regulation of the Notch ligand Delta-like 4 inhibits VEGF-induced endothelial cell function. *Blood* 2006; **107**: 931–939.
38. Sonoshita M, Aoki M, Fuwa H, *et al*. Suppression of colon cancer metastasis by Aes through inhibition of Notch signaling. *Cancer Cell* 2011; **19**: 125–137.
39. Song G, Zhang Y, Wang L. MicroRNA-206 targets notch3, activates apoptosis, and inhibits tumor cell migration and focus formation. *J Biol Chem* 2009; **284**: 31921–31927.
40. Wu Y, Cain-Hom C, Choy L, *et al*. Therapeutic antibody targeting of individual Notch receptors. *Nature* 2010; **464**: 1052–1057.
41. Beatus P, Lundkvist J, Oberg C, *et al*. The notch 3 intracellular domain represses notch 1-mediated activation through Hairy/Enhancer of split (HES) promoters. *Development* 1999; **126**: 3925–3935.
42. Shimizu K, Chiba S, Saito T, *et al*. Functional diversity among Notch1, Notch2, and Notch3 receptors. *Biochem Biophys Res Commun* 2002; **291**: 775–779.
43. Yamaguchi N, Oyama T, Ito E, *et al*. NOTCH3 signaling pathway plays crucial roles in the proliferation of ErbB2-negative human breast cancer cells. *Cancer Res* 2008; **68**: 1881–1888.
44. Meng RD, Shelton CC, Li YM, *et al*. γ-Secretase inhibitors abrogate oxaliplatin-induced activation of the Notch-1 signaling pathway in colon cancer cells resulting in enhanced chemosensitivity. *Cancer Res* 2009; **69**: 573–582.
45. Croner RS, Fortsch T, Bruckl WM, *et al*. Molecular signature for lymphatic metastasis in colorectal carcinomas. *Ann Surg* 2008; **247**: 803–810.
46. Croner RS, Peters A, Brueckl WM, *et al*. Microarray versus conventional prediction of lymph node metastasis in colorectal carcinoma. *Cancer* 2005; **104**: 395–404.
47. Croner RS, Guenther K, Foertsch T, *et al*. Tissue preparation for gene expression profiling of colorectal carcinoma: three alternatives to laser microdissection with preamplification. *J Lab Clin Med* 2004; **143**: 344–351.
48. Ribatti D, Nico B, Vacca A, *et al*. The gelatin sponge–chorioallantoic membrane assay. *Nat Protoc* 2006; **1**: 85–91.
49. Indraccolo S, Gola E, Rosato A, *et al*. Differential effects of angiostatin, endostatin and interferon-alpha(1) gene transfer on *in vivo* growth of human breast cancer cells. *Gene Ther* 2002; **9**: 867–878.
50. Keyaerts M, Verschueren J, Bos TJ, *et al*. Dynamic bioluminescence imaging for quantitative tumour burden assessment using IV or IP administration of D-luciferin: effect on intensity, time kinetics and repeatability of photon emission. *Eur J Nucl Med Mol Imaging* 2008; **35**: 999–1007.

SUPPORTING INFORMATION ON THE INTERNET

The following supporting information may be found in the online version of this article.

Supplementary materials and methods.

Figure S1. Expression of Notch3 transcripts in colon tumours versus normal mucosa by Affymetrix microarray analysis.

Figure S2. Key features of the MICOL14/MICOL-14^{tum} xenografts.

Figure S3. Evaluation of Notch3 levels and Notch activity in MICOL-14 and MICOL-14^{tum} cells *in vitro*.

Figure S4. Activated Notch1 expression in CRC by IHC.

Table S1. Patient characteristics and histopathological features of samples undergoing microarray analysis.

Table S2. Demographics of 177 sequential patients with colon adenocarcinomas (surgery was performed from 1997 to 2000 at the John Radcliffe Hospital, Oxford, UK).

Table S3. Associations between molecular and clinicopathological variables.

Table S4. Univariate analysis of overall survival.

Table S5. Primers used for quantitative or end-point RT-PCR analysis.